

## 5. DATA ANALYSIS

Data analysis consists of characterizing the UWB interference and quantifying the effects of the interference on GPS receiver signal acquisition, signal tracking, and range estimation functions. The effects of UWB interference on signal acquisition and signal tracking are characterized with the BL point and RQT operational metrics. The effects of UWB interference on range estimation are characterized with observational metrics such as the statistics of range error.

### 5.1 UWB Signal Characterization

Band-limited UWB signals can be decomposed into time-varying amplitude and phase functions. Engineers, in the past, have found strong correlation between signal amplitude statistical characteristics and receiver performance. Therefore it should not be surprising that signal amplitude statistical characteristics are suspected as being correlated to GPS receiver performance degradation.

Signal amplitude statistics are often visualized with the APD. The APD shows the probability or percent of time a signal will exceed an amplitude value. Formally:

$$F_A(a) = P(A > a) ,$$

where  $A$  is the amplitude random variable and  $a$  is an amplitude value. The APD is the compliment of the amplitude cumulative distribution function (CDF) which describes the probability a signal amplitude will be less than or equal to an amplitude value. The APD can also be written in terms of the CDF as:

$$F_A(a) = 1 - P(A \leq a) .$$

APDs are often plotted on a Rayleigh graph where the amplitude of Gaussian noise is represented by a negatively sloped, straight line. Gaussian noise mean power corresponds to the power at the 37th percentile.

Non-Gaussian signals have APDs that deviate from the straight line when plotted on a Rayleigh graph. Non-Gaussian signal mean power cannot be read directly from the APD. However, when the power samples are normalized by some reference power, power ratios (peak-to-mean or peak-to-median) can be determined. In addition, the percentage of time a non-Gaussian signal is present can be read from the APD.

The “Gaussian-ness” of the band-limited UWB signal is dependent on the signal pulse repetition frequency and pulse-spacing specifications and the bandwidth of the receiver filter. Figure 5.1.1 shows two UWB signal APDs along with a Gaussian noise APD. The curves are normalized to 0-dBm/20MHz mean power. The first APD corresponds to a UWB signal with a 1-MHz PRF and uniform pulse spacing. The second APD corresponds to a UWB signal with a 1-MHz PRF and 2% relative referenced dithering. Because the PRF is much less than the bandwidth, the pulses are resolved, and the amplitude statistics are nearly identical. Therefore, the two curves lie on top of each other. Both have approximately 10 dB peak to mean power ratios. The pulse is present approximately 60% of the time.

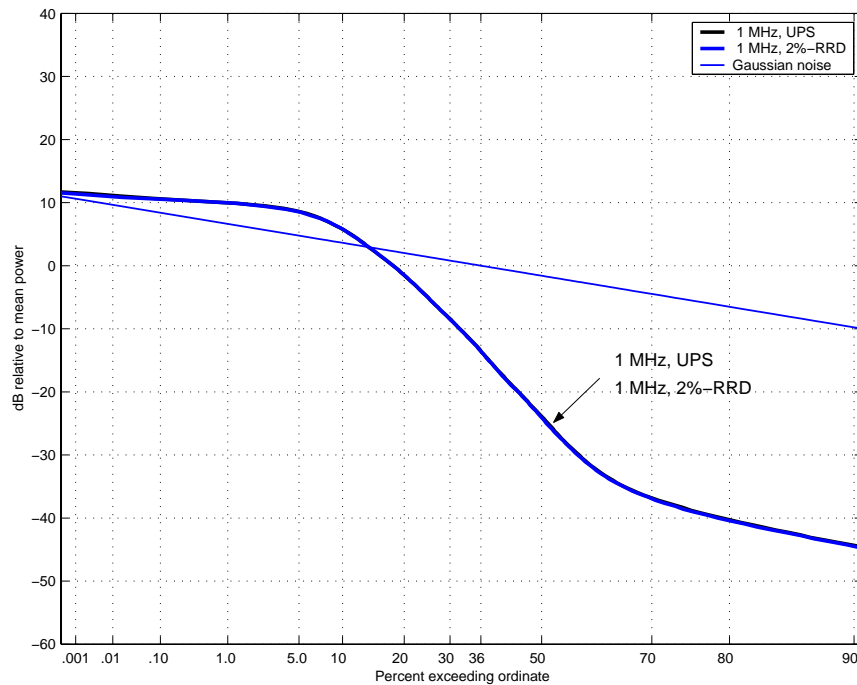


Figure 5.1.1 APDs for Gaussian noise, 1-MHz PRF with UPS, and 1-MHz PRF with 2% RRD.

A complete collection of APDs derived from samples of UWB interferers used during BL and RQT tests can be found in Appendix C. These APDs were acquired with 3 MHz and 20 MHz bandwidths. A detailed tutorial on the APD can be found in Appendix E.

## 5.2 Operational Metrics

### 5.2.1 Break-lock Point

The BL point is the UWB signal power level that causes a receiver in tracking mode to re-enter acquisition mode. For some receivers, BL refers to the failure of C/A code delay tracking while for other receivers, BL refers to loss of carrier phase tracking.

Theoretically BL is a binomially distributed random process - the receiver is either locked or not. Thus BL can occur over a range of UWB signal levels and is likely to vary with BL measurement duration. Rather than assigning a BL point, it would be more accurate to assign a BL probability to every UWB signal level tested. Unfortunately, repeated BL measurements at various power levels and BL measurement durations are not practical.

Thus, for analysis purposes, the BL point is defined to be 1 dB above the maximum UWB signal power, where the receiver is able to maintain lock during the entire BL measurement duration, while the BL test is decrementing. At times, the receiver was able to maintain lock at a UWB signal power when the BL test was incrementing but lost lock at the same level while the BL test was decrementing. In this case the BL point is defined to be 1 dB above this UWB signal power.

### 5.2.2 Reacquisition Time

The RQT is the time it takes a receiver, forced from tracking to acquisition by the sudden removal of the satellite signal, to reenter tracking mode. As in BL, for some receivers tracking refers to the C/A code delay tracking, while for other receivers it refers to the carrier phase tracking.

RQT is assumed to be a Gaussian distributed random variable. However; no test was formally conducted to confirm this. Furthermore, there is a binomially distributed element to the RQT test since RQT measurements are not always successful. A RQT measurement is unsuccessful when reacquisition is not obtained in less than  $RQT_{max}$  seconds. When the measurement is unsuccessful, in principle, no RQT exists.

Rather than ignore the unsuccessful measurement a new random variable was defined:

$$\delta = \min(RQT, RQT_{max}) .$$

The mean  $\bar{b}$  was then used for analysis purposes:

$$m_{\bar{b}} = \frac{1}{N} \sum_{n=1}^N \bar{b}_n ,$$

where  $N$  is the number of RQT measurements.

If all measurements are successful, then mean  $\bar{b}$  is equivalent to the mean RQT. This is no longer true if at least one measurement is unsuccessful. The advantage of using mean  $\bar{b}$  is that it steadily converges to  $RQT_{\max}$  with increasing UWB signal level. In contrast, mean RQT becomes more variable due to the decrease in the number of successful measurements.

### 5.3 Observational Metrics

Range, cycle slip, and SNR observational metrics were derived from data acquired during the BL measurement. Cycle slip and SNR require minimal additional processing. However, range requires a considerable amount of processing to yield useful analysis information.

#### 5.3.1 Range Performance

Degradation of the range estimate is determined by analysis of range error statistics. Range error values were derived from subtracting a known, simulated range from the range measured by the GPS receiver. The range error statistic was found to be time dependant and therefore non-stationary. This non-stationarity was introduced by systematic errors due to the GPS radio environment and spectral line interference. A calibration and correction procedure was developed to remove the systematic component, giving a range error residual – the statistics of which were then used for analysis.

#### Range

Two range estimates – pseudorange (PSR) and accumulated delta-range (ADR) – were derived from observables sampled during the BL measurement. PSR is the most fundamental range measurement derived from correlation of the C/A code. The prefix *pseudo* highlights the fact that satellite and receiver clocks are not synchronized. ADR is an ambiguous range corresponding to the accumulated differences in range from one time to another. ADR is derived from observation of the Doppler-shifted radio frequency carrier. Although the ADR is ambiguous, it has much less uncertainty than PSR. This ambiguity can be resolved with a time-averaged code-minus-carrier (CMC) range bias which is defined to be the difference between the PSR and ADR.

Fundamentally, PSR (m) is defined by

$$D = c(t_u - t_s) \quad ,$$

where  $c$  is the speed of propagation (m/s),  $t_u$  is the received time (s), and  $t_s$  is the transmitted time. An alternative expression for PSR is

$$D(t) = |\mathbf{r}_s(t) - \mathbf{r}_u(t)| - r_D(t) \quad ,$$

where bold letters represent vectors,  $\mathbf{r}_s$  is the position of the satellite,  $\mathbf{r}_u$  is the position of the user receiver,  $|\mathbf{r}_s - \mathbf{r}_u|$  is the geometric range between the two positions, and  $r_D$  is the PSR error (m).

ADR is derived from the delta-PSR (DPSR) velocity measurement. The DPSR is defined by the rate of change of PSR (m/s)

$$\dot{D}(t) = [\mathbf{v}_s(t) - \mathbf{v}_u(t)] \cdot \mathbf{I}(t) - \dot{r}_D(t) \quad ,$$

where  $\mathbf{v}_s$  is the velocity of the satellite (m/s),  $\mathbf{v}_u$  is the velocity of the receiver,  $\dot{r}_D$  is the DPSR error, and  $\mathbf{I}$  is the unit range vector between the satellite and the receiver defined by

$$\mathbf{I}(t) = \frac{\mathbf{r}_s(t) - \mathbf{r}_u(t)}{|\mathbf{r}_s(t) - \mathbf{r}_u(t)|} \quad .$$

DPSR can also be expressed as a function of Doppler frequency shift  $D$  (Hz) since

$$\dot{D}(t) = \frac{c}{\lambda} [\mathbf{v}_s(t) - \mathbf{v}_u(t)] \cdot \mathbf{I}(t) \quad ,$$

where  $\lambda$  is the carrier frequency wavelength (m). Substitution gives

$$\dot{D}(t) = \dot{D}(t) - \dot{r}_D(t) \quad .$$

Integrating DPSR yields ADR formally defined as

$$ADR(t_1, t) = \int_{t_1}^t \dot{D}(J) dJ = |\mathbf{r}_s(t) - \mathbf{r}_u(t)| - r_{D,ADR}(t) \quad ,$$

where  $t_1$  is the integration starting time and ADR error is related to DPSR error via

$$r_{D,ADR}(t_1, t) = \int_{t_1}^t \dot{r}_D(J) dJ \quad ,$$

Finally, CMC is formally defined as

$$\chi(t_1, t) = \rho(t) - \alpha(t_1, t) \quad .$$

CMC minimizes systematic errors common to both PSR and ADR and helps isolate the effects of interference.

Examples of simulated PSR, DPSR, ADR, and CMC are shown in Figure 5.3.1.1. These parameters are taken from the simulator “log” file which provides true range data used to calculate range error in the next section. Simulation time is the time from the start of the simulation. PSR is from approximately  $20.4 \times 10^6$  m to  $20.8 \times 10^6$  m. The satellite is at zenith when the PSR is a minimum at approximately 1300 s. DPSR is a relatively straight line with negative velocities as the satellite approaches and positive velocities as it recedes. The DPSR is 0 m/s at zenith corresponding to a 0-Hz Doppler shift. ADR is 0 m at the start of the simulation. The ADR decreases as the satellite approaches and increases as the satellite recedes. The ADR curve is similar to the PSR curve without the initial range offset. CMC is constant at this offset from start to finish.

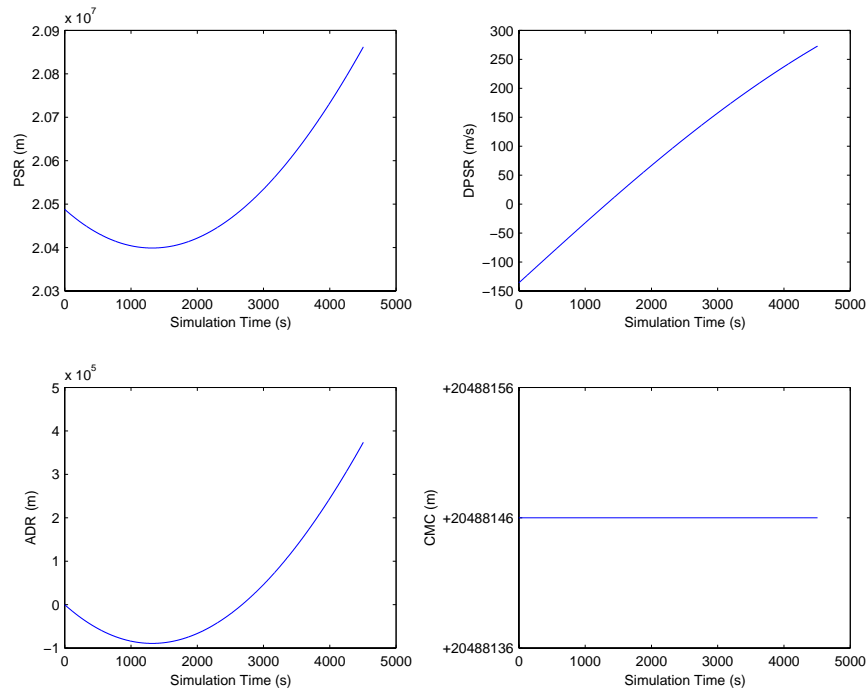


Figure 5.3.1.1 Simulated values.

## Range Error

Measured ranges have more sources of error than simulated ranges [5, 6]. For example, measured PSR is represented by

$$\hat{\rho}(t) = |\mathbf{r}_s(t) - \mathbf{r}_u(t)| + c\hat{b}_u(t) + \hat{\epsilon}_p(t) ,$$

where  $\hat{\cdot}$  denotes measured values and  $b_u$  is the receiver clock offset (s). This expression demonstrates that measured ranges are influenced by receiver noise and clock inaccuracies. These error sources are also present in DPSR as expressed by

$$\hat{\delta}(t) = \lambda\hat{D}(t) + c\frac{d\hat{b}_u(t)}{dt} + \hat{\epsilon}_\delta(t) ,$$

and consequently ADR. Computation of ADR alone sometimes requires compensation of the clock offset for Doppler effects. Computation of ADR for CMC does not require this compensation because these effects are also present in PSR.

Examples of measured PSR, DPSR, ADR, and CMC are shown in Figure 5.3.1.2. These parameters were measured using Rx 1 with -93 dBm/20MHz Gaussian noise added to the GPS signal. The measured ranges are different from the simulated ranges in Figure 5.3.1.1. CMC shows measurement uncertainty most dramatically because systematic error was removed.

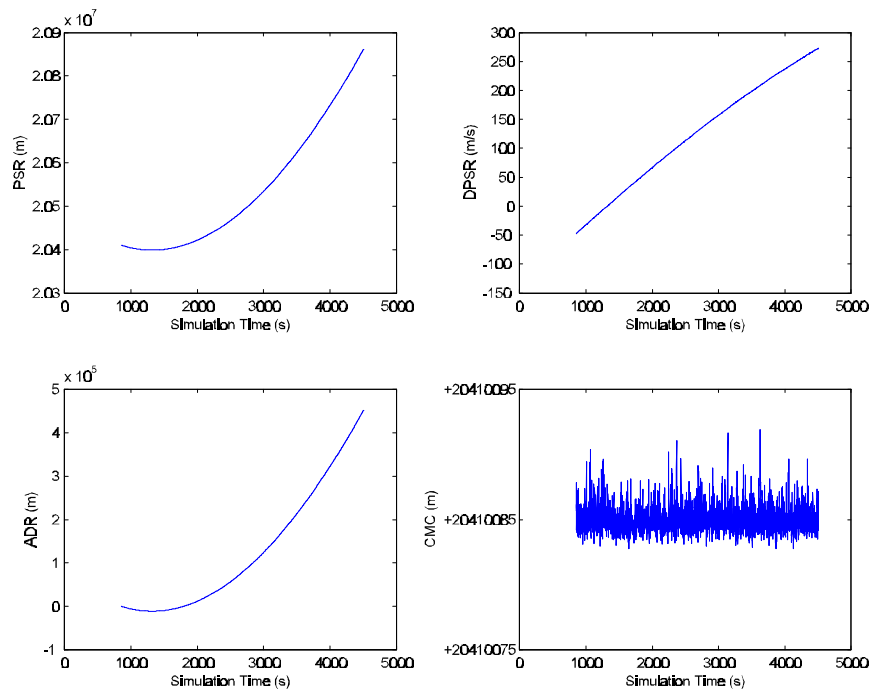


Figure 5.3.1.2 Reference measurement values.

Range error is the difference between simulated and measured range estimates. PSR error is

$$\Delta_p(t) = \hat{\rho}(t) - c \hat{b}_u(t) - \rho(t) = \hat{\epsilon}_\rho(t) - \epsilon_\rho(t) ,$$

ADR error is

$$\Delta_\alpha(t_1, t) = \hat{\alpha}(t_1, t) - \alpha(t_1, t) = \hat{\epsilon}_\alpha(t_1, t) - \epsilon_\alpha(t_1, t) ,$$

and CMC error is

$$\Delta_\chi(t_1, t) = \hat{\chi}(t_1, t) - \chi(t_1, t) = [\hat{\epsilon}_\rho(t) - \epsilon_\rho(t)] - [\hat{\epsilon}_\alpha(t_1, t) - \epsilon_\alpha(t_1, t)] .$$

Figure 5.3.1.3 shows range error corresponding to the simulated and measured ranges in Figures 5.3.1.1 and 5.3.1.2. Notice that PSR and ADR cases have curved features while the CMC case is relatively flat. The curves are indicative of an underlying non-stationary process where the range-error statistic is dependent on time. This non-stationarity is undesirable and must be minimized before more detailed statistical analysis can proceed.

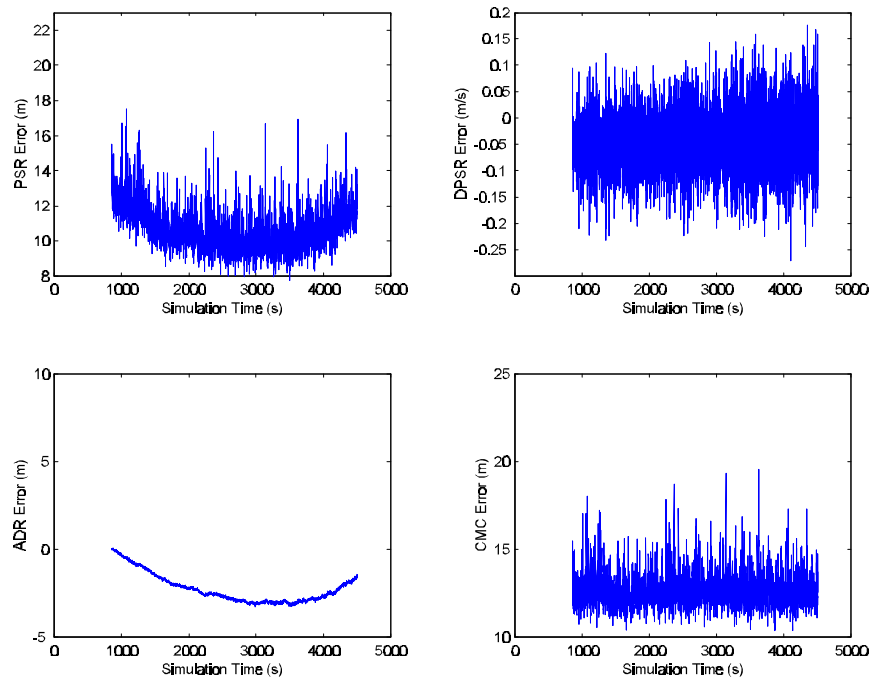


Figure 5.3.1.3 Reference range error.

## Range error residual

In order to separate the effects of UWB interference, a general expression for range error is

$$\hat{r}_{ref} = r_{ref} + \hat{\epsilon}_{UWB} \quad (5.3.1.1)$$

where the  $r_{ref}$  is the reference range error and  $\hat{\epsilon}_{UWB}$  is error introduced by UWB interference. We measure  $r_{ref}$  under nominal SNR conditions specified in Table 4.1.1. Figures 5.3.1.2 and 5.3.1.3 show the reference range and reference range error for Rx 1, respectively.

The reference range error can be modeled as

$$r_{ref} = M_{ref} + n_{ref} \quad (5.3.1.2)$$

where  $M_{ref}$  represents the non-stationary systematic reference error and  $n_{ref}$  represents the random reference error and contains high-order components of  $r_{ref}$ .  $M_{ref}$  is a function derived from a 3<sup>rd</sup> order polynomial fit to  $r_{ref}$ . Figures 5.3.1.4 and 5.3.1.5 show these errors for Rx 1. Subtracting  $M_{ref}$  from  $r_{ref}$  removes non-stationary systematic error and yields a range error residual

$$\hat{r}_{ref} = r_{ref} - M_{ref} + \hat{\epsilon}_{UWB} + n_{ref} \quad (5.3.1.3)$$

which is our best estimate to range error due to UWB interference.

Figures 5.3.1.6 and 5.3.1.7 show systematic along with measured range error for two different UWB interference signals. The first is 1-MHz PRF with UPS and no gating. The second is 1-MHz PRF with 2% RRD and no gating. In both cases, Rx 1 was exposed to the maximum UWB power levels where lock is maintained. The UPS case has spectral line interference starting at 2000 seconds. PSR, ADR, and CMC show significant changes in error at this point. Prior to this spectral alignment, the error coincides with  $M_{ref}$ . The 2% RRD case has an elevated range error when compared to  $M_{ref}$ .

Figures 5.3.1.8 and 5.3.1.9 show the range error residuals for these same UWB signals. Clearly the magnitude of the residuals is less. The increased error due to spectral line interference is still dominant in the UPS case.

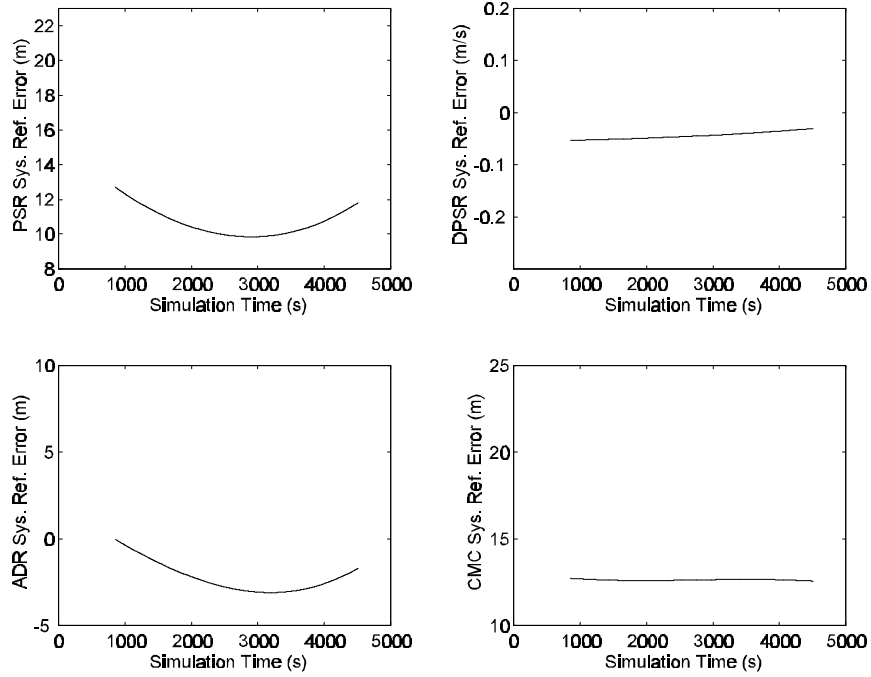


Figure 5.3.1.4 Systematic reference error ( $M_{ref}$ ).

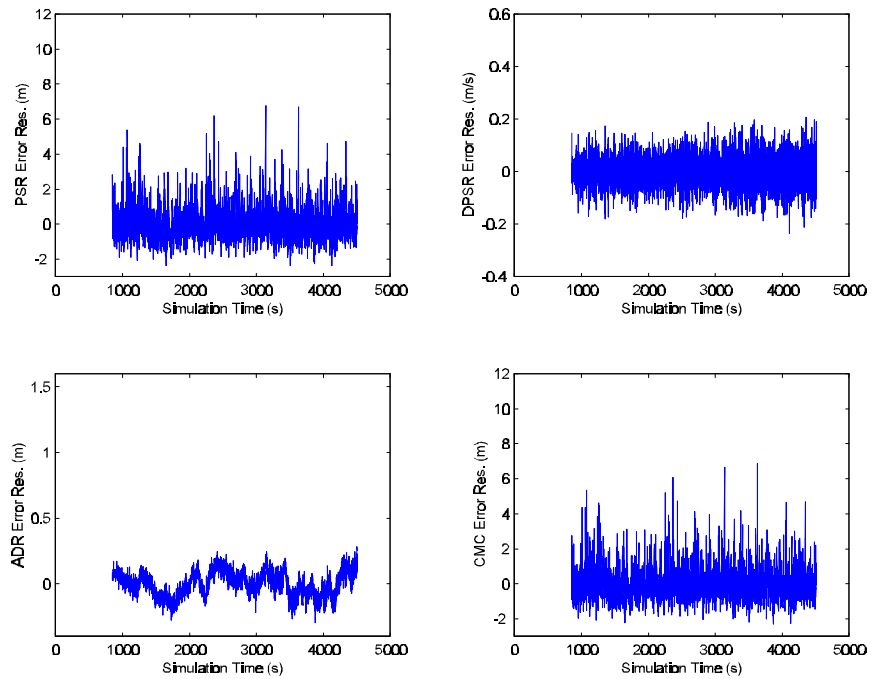


Figure 5.3.1.5 Random reference error ( $n_{ref}$ ).

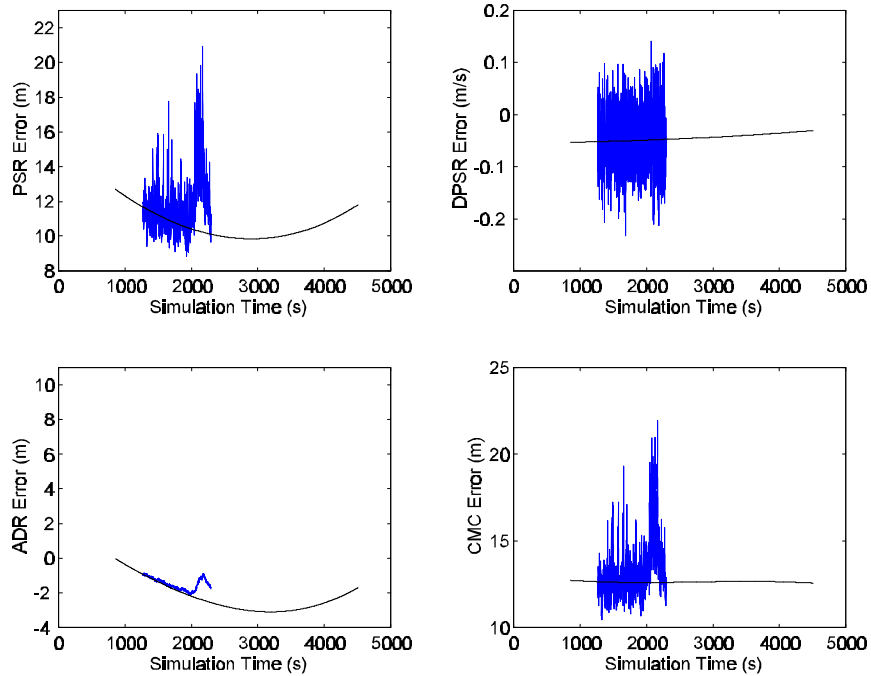


Figure 5.3.1.6 Range error due to 1-MHz PRF with UPS interference compared to systematic reference range error.

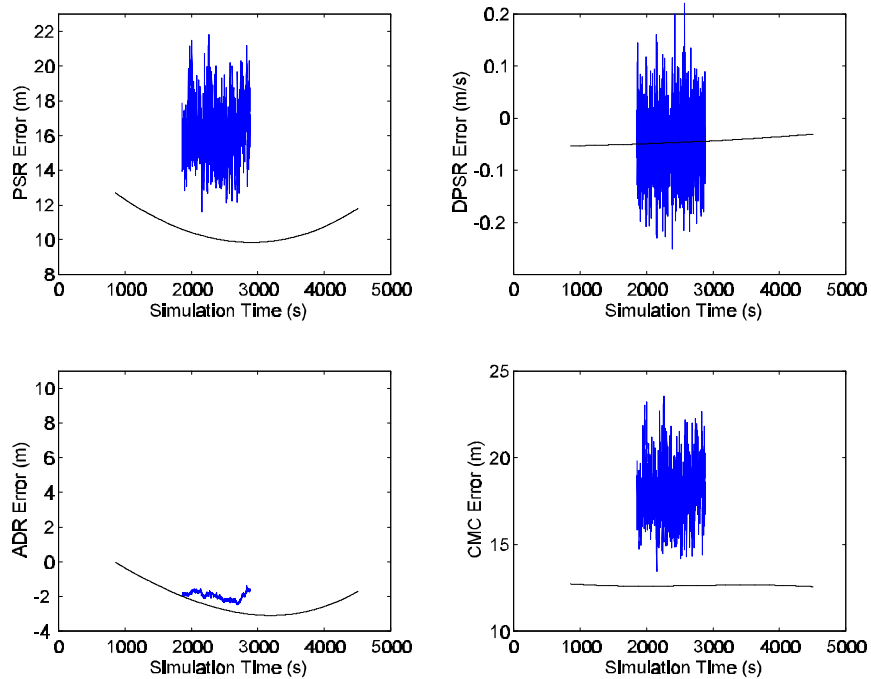


Figure 5.3.1.7 Range error due to 1-MHz PRF with 2%-RRD interference compared to systematic reference range error.

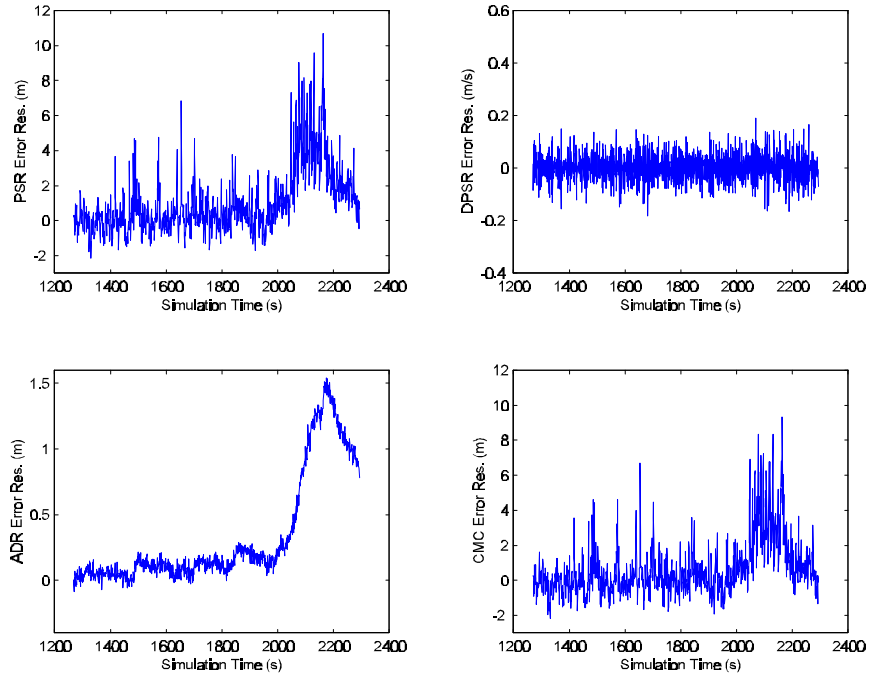


Figure 5.3.1.8 Range error residual due to 1-MHz PRF with UPS interference.

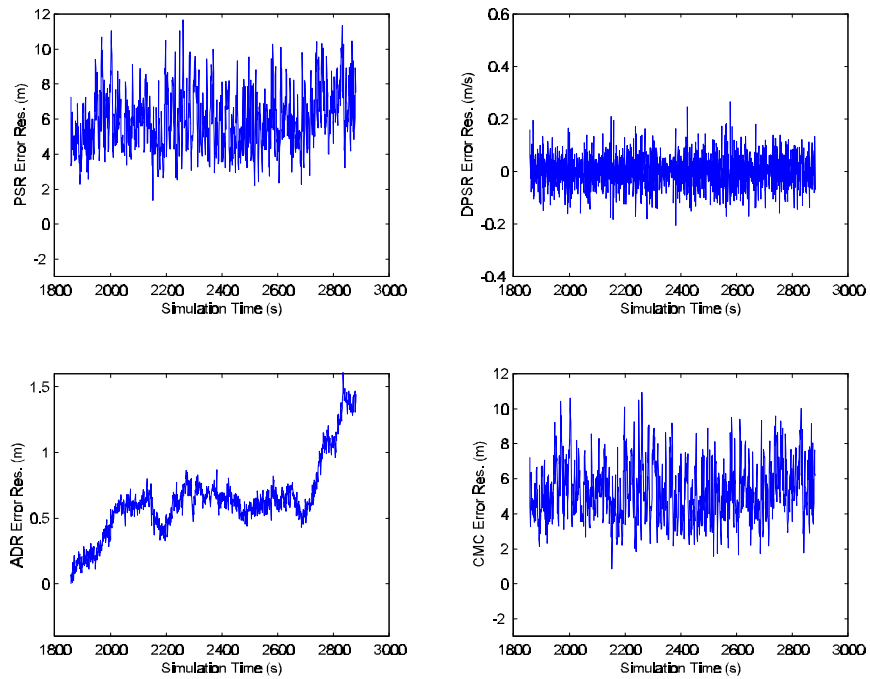


Figure 5.3.1.9 Range error residual due to 1-MHz PRF, 2%-RRD interference.

## Range error residual statistics

The range error residual is analyzed with numerous statistics. Range error residual standard deviation is a commonly used statistic for evaluating the effect of interference. Zero-mean, Gaussian distributed random variables are completely described by the standard deviation statistic

$$F_c = \sqrt{\frac{1}{N} \sum_{n=1}^N (c_n - m_c)^2}$$

where  $N$  is the number of range error residual samples and  $m$  is the mean range error residual. Although this statistic was evaluated, it was deemed insufficient because the range error residuals were often non-Gaussian. Therefore, in addition to standard deviation, other statistics including percentiles were analyzed [7].

Percentiles are computed from the CDF defined by

$$F_c(c) = P(\# \leq c)$$

where  $c$  is the range error residual random variable. The CDF is most easily obtained by sorting the sampled  $c$  into ascending values. The probability corresponds to the position in the sorted array. The median, 84th, and 98th percentiles represent the range error residual value that are greater than or equal to all others 50, 84, and 98% of the time. The 84th and 98th percentiles are significant because they represent the 1 and 2 standard deviation values for a zero-mean Gaussian distributed random variable.

Figures 5.3.1.10, 5.3.1.11, and 5.3.1.12 show the range error residual CDFs of the reference measurement and the two 1-MHz PRF cases described above. These CDFs are plotted on a Gaussian graph where a Gaussian distributed random variable is represented by a positively sloped, straight line. The UPS case deviates from this line at approximately the 84th percentile. This percentile corresponds to the time the spectral line interference is present during the BL measurement. The CDF of the 2% RRD case appears Gaussian. The percentiles for PSR and CMC track each other in both cases. This is to be expected since CMC error is dominated by PSR error.

The skewness, excess, and median-to-mean ratio statistics quantify the ‘‘Gaussian-ness’’ of the range error residual. The skewness measures the symmetry of a probability density function and is defined by

$$S_1 = \frac{1}{F^3} \sqrt{\frac{1}{N} \sum_{n=1}^N (c_n - m_c)^3}$$

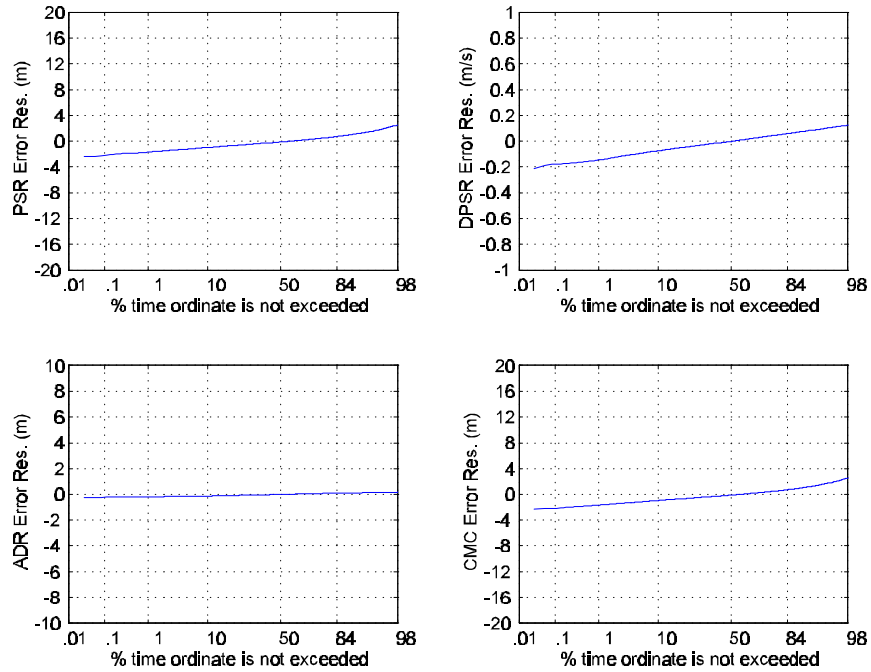


Figure 5.3.1.10 Reference range error residual CDF.

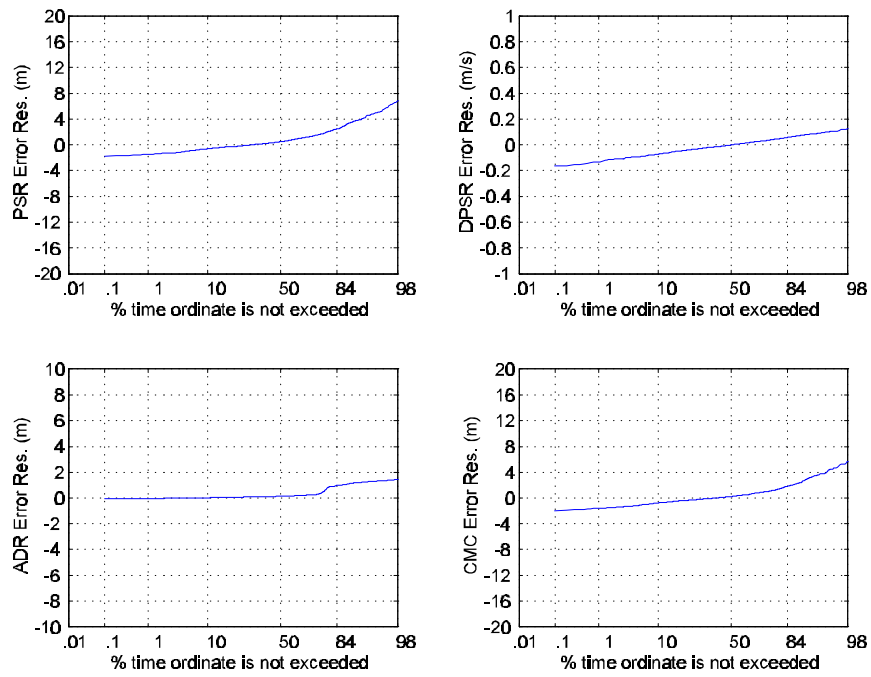


Figure 5.3.1.11 Range error residual CDF for 1-MHz PRF with UPS interference measurement.

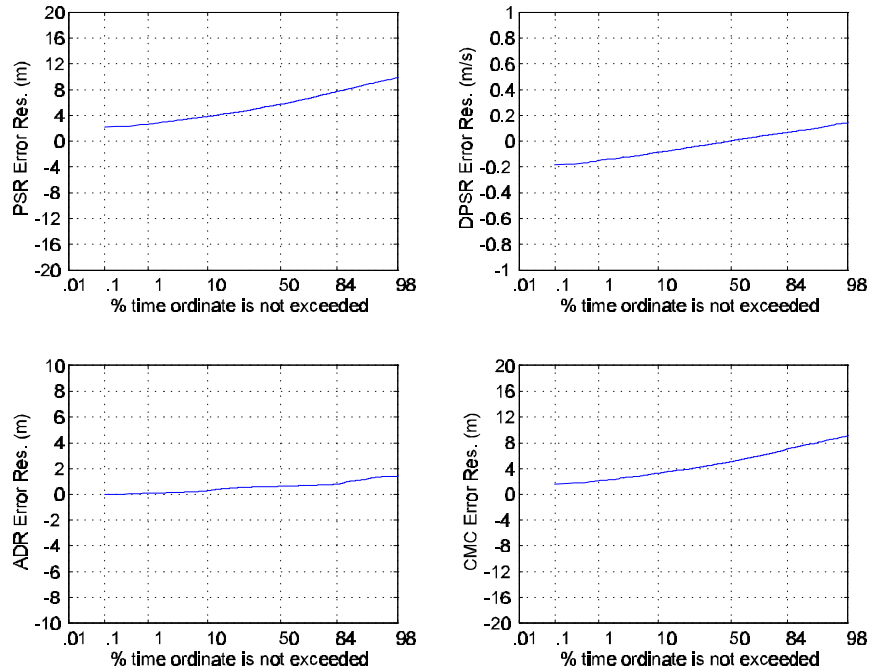


Figure 5.3.1.12 Range error residual CDF for 1-MHz PRF with 2% RRD interference measurement.

Gaussian distributed random variables have a skewness of 0. The excess measures the “peakedness” of a random variable and is defined by

$$\beta_2 = \frac{1}{\sigma^4} \sqrt{\frac{1}{N} \sum_{n=1}^N (\gamma_n - m_\gamma)^4} .$$

Gaussian distributed random variables have an excess of 3. A Gaussian distributed random variable has a median-to-mean ratio of 1. For display, 3 is subtracted from excess and 1 is subtracted from the median-to-mean ratio so they, like skewness, will be centered at zero. Deviations from zero for any of these statistics will indicate that the random variable is non-Gaussian.

Range error residual standard deviation estimates are unreliable if there are too few independent samples. The auto-correlation function is used to evaluate the independence of the range error residual samples:

$$R_\Gamma(k) = \frac{1}{N} \sum_{n=1}^N (\gamma_n - m_\gamma)(\gamma_{n+k} - m_\gamma) ,$$

where  $m_\zeta$  represents the mean residual error and  $N$  is the number of residual error samples. The number of correlated samples is the smallest value of  $k$  whose autocorrelation is less than  $R(0)/2$ . ADR error residuals were typically highly correlated because ADR is the result of integrating DPSR. Figures 5.3.1.13, 5.3.1.14, and 5.3.1.15 show the autocorrelation function of the reference measurement, UPS case, and 2% RRD case. The reference measurement and 2% RRD case show clear independence between observations. The UPS case shows more correlation corresponding to the length of time spent with and without line interference.

### 5.3.2 Cycle Slip and Signal-to-Noise Ratio

To our knowledge, the receivers that were tested do not count or estimate the actual number of cycle slips. Instead, the receivers monitor parameters that are correlated to cycle slip conditions (e.g., SNR, carrier phase lock, and bit error rates).

Cycle slip condition is a binomially distributed random variable, being either present or not. Analysis consists of counting the number of observations where cycle slip conditions are present and dividing by the total number of observations. This fraction represents cycle slip condition probability which is converted to percentage for display.

Figures 5.3.2.1a and 5.3.2.2a show cycle slip condition probability for the two 1-MHz PRF cases described above. The UPS case has the majority of cycle slip conditions clustered around the time when line interference is strongest. For the 2% RRD case, cycle slip conditions are scattered uniformly throughout the entire measurement.

SNR is analyzed in percentiles in a similar manner to the range error residual. The occurrence of low SNR is of interest thus the 50th, 16th, and 2nd percentiles are displayed. Figures 5.3.2.1b and 5.3.2.2b show SNR behavior for the two 1-MHz PRF cases. As expected, the UPS case has degraded SNR around the time when line interference is strongest. The 2% RRD case has small degradations in SNR throughout the entire measurement.

It should be noted that GPS receiver SNR measurements may not be accurate when the band-limited UWB signal has non-Gaussian statistics. The designer of the GPS noise measurement circuitry may have assumed, for example, that the noise would have Gaussian statistics. Thus, the SNR threshold for cycle slip conditions may need to be adjusted for non-Gaussian noise.

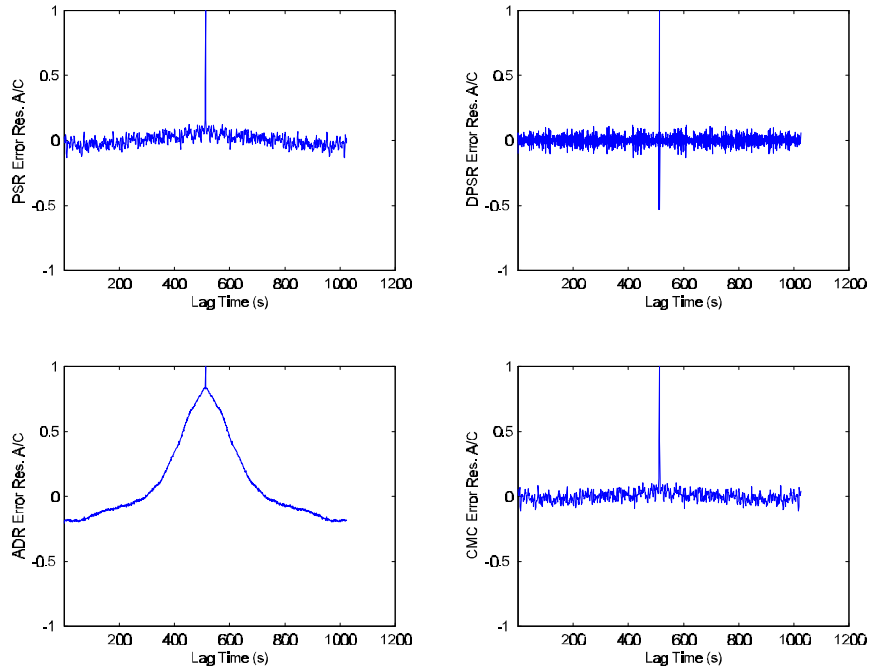


Figure 5.3.1.13 Autocorrelation of reference range error residual.

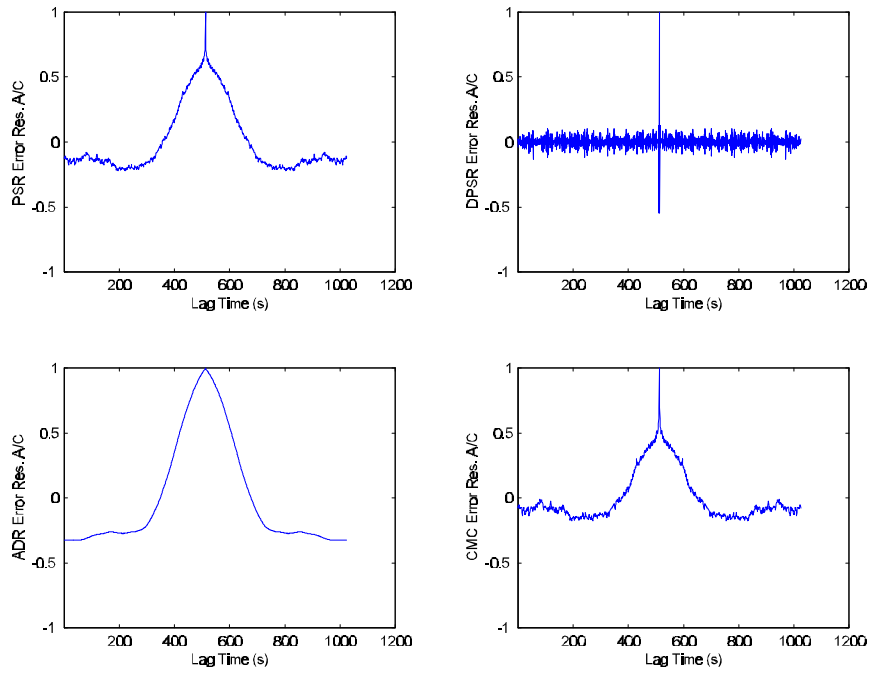


Figure 5.3.1.14 Autocorrelation of range error residual for 1-MHz PRF with UPS interference measurement.

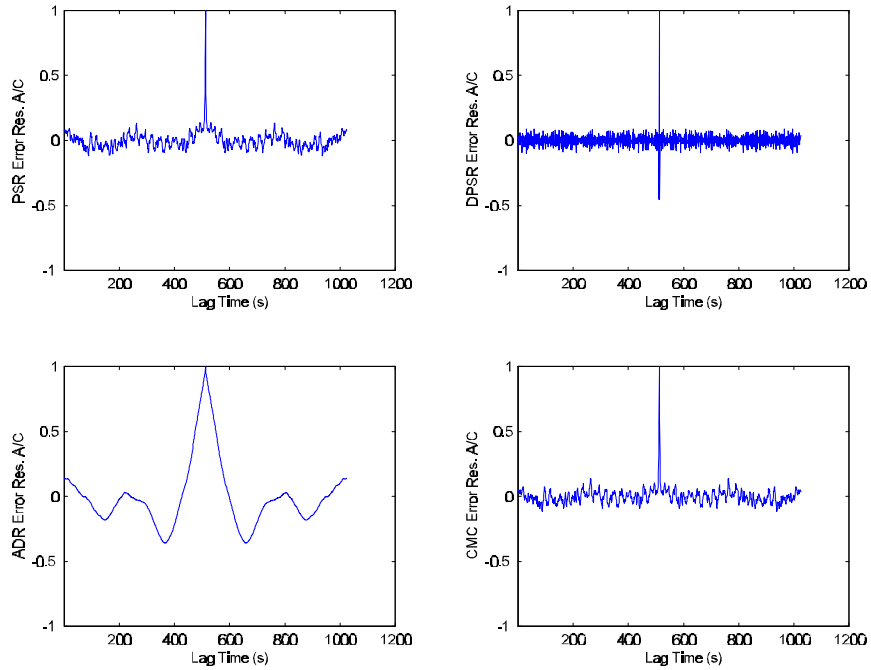


Figure 5.3.1.15 Autocorrelation for 1-MHz PRF with 2%-RRD interference measurement.

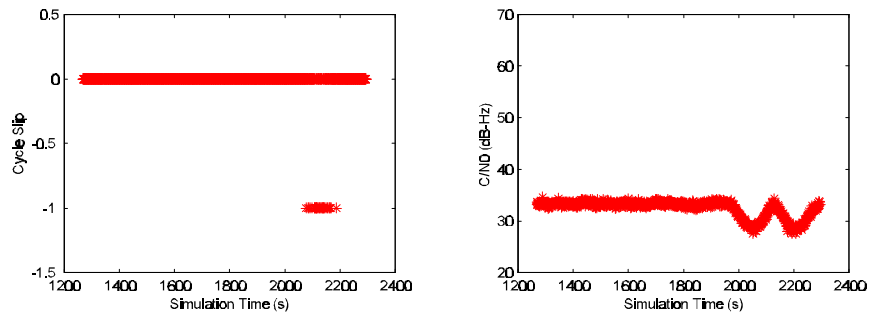


Figure 5.3.2.1 Cycle slips and SNR for 1-MHz PRF with UPS interference measurement.

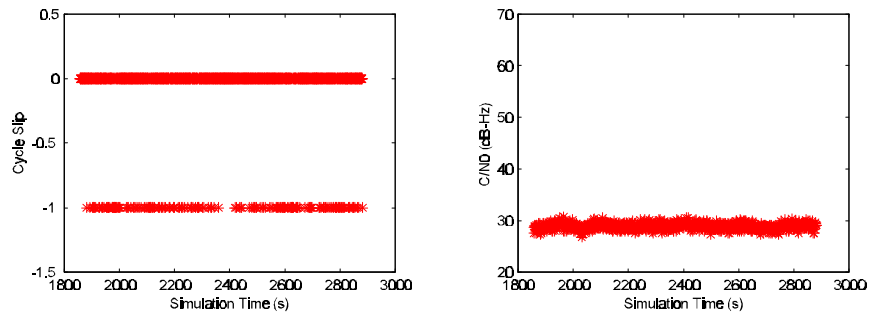


Figure 5.3.2.2 Cycle slips and SNR for 1-MHz PRF with 2%-RRD interference measurement.

## 5.4 Uncertainty Analysis

Four random variables are estimated through measurement: BL point, RQT, range error, and probability of cycle slip conditions. Discussion of the uncertainty of these estimates is as important as the estimates themselves.

Uncertainty is often quoted in terms of accuracy and precision. An accurate estimate implies that the mean is close to the true value. A precise estimate implies that the variation about the mean is minimal. Another way of expressing uncertainty is to define a random interval along with a probability or confidence that the random interval will include the true value [8].

### 5.4.1 Break-lock Point

BL point was found to occur as much as 4 dB below the UWB signal level that first caused BL. A test using Gaussian noise with Rx 1 showed that it was possible to have successful and unsuccessful BL measurements over a 4-dB range. Below this range BL was seldom experienced with repeated trials. Above this range BL was frequently experienced with repeated trials. Thus, it can be said that the BL point variability is approximately  $\pm 2$  dB.

### 5.4.2 RQT

RQT is assumed to be Gaussian distributed. However, since there are a limited number of RQT trials the Student-t distribution is used for computational purposes. Formally, if the number of trials is fixed at 10, the confidence interval for 95% confidence is

$$m - 0.76s \leq u < m + 0.76s \quad ,$$

where  $u$  is the true mean,  $m$  is the measured mean, and  $s$  is the measured standard deviation. This uncertainty estimate is only valid when all trials had successful reacquisitions. RQT trials are considered independent because the receiver was reset at the beginning of each measurement.

### 5.4.3 Range Error

The standard deviation of the range error residual,  $F_{\text{uere}}$ , (user-equivalent range error) is an important factor in the GPS error budget. The uncertainty of a laboratory estimate of  $F_{\text{uere}}$  is often expressed as a confidence interval. If there are 1024 independent observations and the underlying process is Gaussian distributed, the standard deviation interval for 95% confidence is

$$0.9585s \leq \sigma < 1.045s \quad ,$$

where  $s$  is the measured range error residual standard deviation, and  $F$  is the true range error residual standard deviation. Range error residual confidence intervals cannot be computed for UWB signals with spectral line interference because their statistics are non-Gaussian.

#### **5.4.4 Cycle Slip Conditions**

For Rx 1, cycle slip conditions do not cause loss of lock. Thus it was possible to collect a number of cycle slip condition samples during a single BL measurement. Although it is practical to compute the uncertainty of this random variable it is unclear how independent the cycle slip condition samples are. For example, if the cycle slip condition is detected with a message parity error it may take several seconds to clear the cycle slip condition indicator. Since cycle slips condition is used to support other trends it was deemed unnecessary to analyze the uncertainty of cycle slip condition probability.